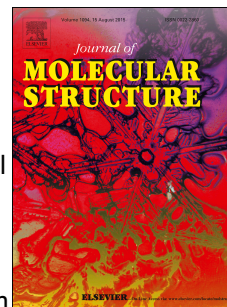


Accepted Manuscript

Synthesis, characterization, photoluminescence, and electrochemical studies of novel mononuclear Cu(II) and Zn(II) complexes with the 1-benzylimidazolium ligand

Sherino Bibi, Sharifah Mohammad, Ninie Suhana Abdul Manan, Jimmy Ahmad, Muhammad Afzal Kamboh, Sook Mei Khor, Bohari M. Yamin, Siti Nadiah Abdul Halim



PII: S0022-2860(17)30359-9

DOI: [10.1016/j.molstruc.2017.03.072](https://doi.org/10.1016/j.molstruc.2017.03.072)

Reference: MOLSTR 23568

To appear in: *Journal of Molecular Structure*

Received Date: 4 January 2017

Revised Date: 17 March 2017

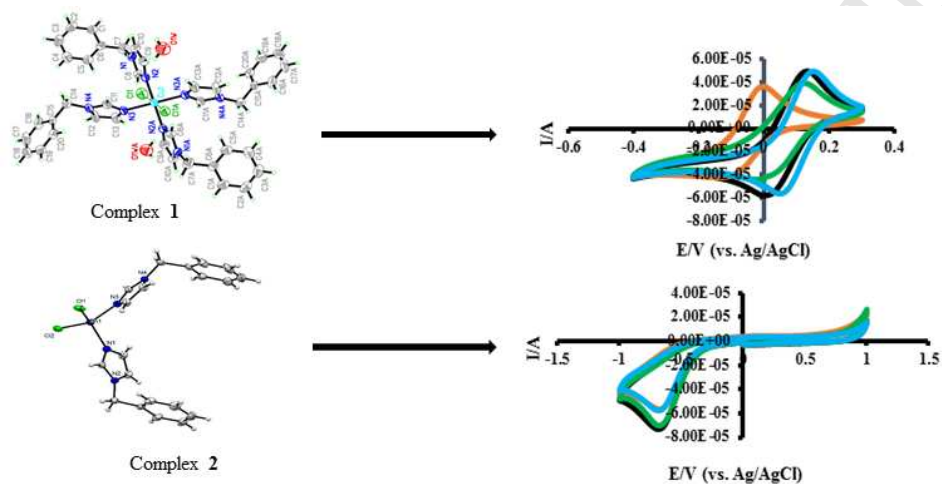
Accepted Date: 19 March 2017

Please cite this article as: S. Bibi, S. Mohammad, N.S.A. Manan, J. Ahmad, M.A. Kamboh, S.M. Khor, B.M. Yamin, S.N. Abdul Halim, Synthesis, characterization, photoluminescence, and electrochemical studies of novel mononuclear Cu(II) and Zn(II) complexes with the 1-benzylimidazolium ligand, *Journal of Molecular Structure* (2017), doi: 10.1016/j.molstruc.2017.03.072.

This is a PDF file of an unedited manuscript that has been accepted for publication. As a service to our customers we are providing this early version of the manuscript. The manuscript will undergo copyediting, typesetting, and review of the resulting proof before it is published in its final form. Please note that during the production process errors may be discovered which could affect the content, and all legal disclaimers that apply to the journal pertain.

Graphical abstract

Two novel coordination complexes $[\text{Cu}(\text{bim})_4\text{Cl}_2] \cdot 2\text{H}_2\text{O}$ (**1**) and $[\text{Zn}(\text{bim})_2\text{Cl}_2]$ (**2**) based on benzylimidazole have been synthesized and structurally characterized. The electrochemical behavior of the title complexes has been investigated in 4 different electrolytes.



Synthesis, characterization, photoluminescence, and electrochemical studies of novel mononuclear Cu(II) and Zn(II) complexes with the 1-benzylimidazolium ligand

Bibi Sherino^{a,b}, Sharifah Mohammad^a, Ninie Suhana Abdul Manan^{a,c}, Jimmy Ahmad^a, Muhammad Afzal Kamboh^e, Sook Mei Khor^a, Bohari M Yamin^d, and Siti Nadiyah Abdul Halim^{a*}

^a*Department of Chemistry, Faculty of Science, University of Malaya, 50603 Kuala Lumpur, Malaysia*

^b*Department of Chemistry, Sardar Bahadur Khan Women University, Quetta, Balochistan, Pakistan*

^c*Center For Ionic Liquids (UMCiL), 50603 University Malaya Kuala Lumpur, Malaysia*

^d*School of Chemical Sciences and Food Technology, University Kebangsaan Malaysia*

^e*School of Chemistry, Shaheed Benazir Bhutto University Shaheed, Benazirabad, Sindh, Pakistan*

Abstract

Two new mononuclear coordination complexes [Cu(bim)₄Cl₂]·2H₂O (**1**) and [Zn(bim)₂Cl₂] (**2**) containing the 1-benzylimidazole (bim) ligand were successfully synthesized. Both complexes were characterized by IR, UV-vis, and fluorescence spectroscopies, single crystal and powder X-ray diffraction measurements, and thermogravimetric analysis. Self-assembly during the recrystallization process resulted in the formation of octahedral and tetrahedral Cu(II) and Zn(II) complexes, respectively. The single crystals obtained are representative of the bulk material, as shown by the powder X-ray diffraction patterns. Cyclic voltammetry measurements showed that complex **1** undergoes a quasi-reversible redox reaction, while complex **2** undergoes reduction alone, and no oxidation peak was observed; this is due to the stability of the reduced form of complex **2**.

Keywords: synthesis; Cu(II) complex; Zn(II) complex; benzylimidazole; crystal structure.

Author to whom correspondence should be addressed Dr. Siti Nadiyah Abdul Halim (UM), Tel: +603-79674248/+6019-3363554; Fax: +603-79674193; email: nadiyahhalim@um.edu.my

1. Introduction

Recently, coordination complexes have become attractive for use in the production of medicines and drugs, primarily because most metals and organic compounds have some biological activity, such as antifungal agents, antibiotics, and anticancer [1, 2]. However, coordination complexes also have physical and chemical applications, such as in catalysis, luminescence, hydrometallurgy, and sensors [3-5]. In addition, coordination complexes have been widely used in electrochemical studies because of the different oxidation state of transition metal [6, 7].

Coordination complexes contain ligands, which can be ions or neutral molecules, that have lone pairs that can be donated to the central metal atom [8, 9]. The ligand can be varied by the donor atom, for example, N, S, O, or P in phosphines [10], alkoxides, imides [11], phosphoramidites [12], and more [13]. Benzylimidazole is a popular N-donor ligand often used in coordination chemistry. The imidazole ring of benzylimidazole is an important component of numerous natural products, including purine, histidine, histamine, and nucleic acids. The exposed imidazole nitrogen atom of benzylimidazole (shown in **Figure 1**) can bind as a monodentate ligand to a central metal atom [14, 15]. Benzylimidazole is also known to be good Lewis base and metal coordinator because of its pK_a value (approximately 7), and the rotational freedom around the C-N bond in benzylimidazole (shown in **Figure 1**, blue color) allows changes in molecular conformation that lead to distinct coordination compound structures [16-18]. A large number of d-block transition metal and imidazole complexes and their derivatives are known to have biological and physiochemical properties [19], and the coordination capability of a number of monodentate benzylimidazole derivatives [20, 21].

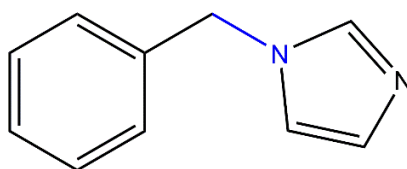


Fig.1. Structure of benzylimidazole.

In this paper, we explore two novel crystal structures of benzylimidazole-based complexes: $[\text{Cu}(\text{bim})_4\text{Cl}_2] \cdot 2\text{H}_2\text{O}$ (**1**) and $[\text{Zn}(\text{bim})_2\text{Cl}_2]$ (**2**). The $[\text{Zn}(\text{bim})_2\text{Cl}_2]$ (**2**) complex has

been previously reported by Pettinari and coworkers, although no crystal structure [22]. Therefore, here, we report the synthesis, spectroscopic characterization, single crystal structure, X-ray diffraction (XRD) measurements, and thermogravimetric (TGA) analysis of complexes **1** and **2** and their electrochemical behavior. The electrochemical studies of both complexes were carried out using cyclic voltammetry (CV).

2. Experimental

2.1. Materials and measurements

1-Benzylimidazole (Sigma–Aldrich, 99%) CuCl₂·2H₂O (98%; R&M chemicals), ZnCl₂ (98%; R&M chemicals). Deionized water (DI) was used as the working solution. All reagents are commercially available and were used without further purification.

The IR spectra were recorded on a Perkin-Elmer 400 FTIR Fourier transform spectrometer (FT-FIR) between 200 and 4000 cm⁻¹. UV-vis spectra were measured using UV-1800 Shimadzu UV-vis spectrometer (200–800 nm), and fluorescence spectra were measured using a JASCO FP-6500 spectrofluorometer.

Powder X-ray diffraction (PXRD) patterns were recorded on a PANalytical X'Pert Pro diffractometer using Cu-K α radiation ($\lambda = 1.541874\text{\AA}$) in the 2θ range of 5 to 40° with a slit size = 0.4785°. Comparison between the experimental and PXRD patterns, calculated from the single-crystal structures, was performed using X'Pert High Score Plus.

X-ray single crystal data for complexes **1** and **2** were collected at 304(4) and 293(2) K on a Bruker AXS SMART APEX II diffractometer with a CCD area detector (Mo K $\alpha = 0.71073\text{\AA}$, monochromator = graphite). High-quality crystals were chosen under a polarizing microscope and mounted on a glass fiber. Data processing and absorption correction were accomplished using the APEXII software package [23]. The structures were solved by direct methods using ShelXS. Hydrogen atoms were placed in geometrically constrained positions and included in the refinement process using riding model with $U_{\text{iso}} = 1.2U_{\text{eq}}$ C (H, H) groups. All the data were refined with full matrix least-squares refinement against $|F^2|$ using ShelXL, and the final refinement includes the atomic position for all the atoms, anisotropic thermal parameters for all the non-hydrogen atoms, and isotropic thermal parameters for all the hydrogen atoms.

Thermogravimetric analysis (SII TG/DTA 6300) was carried out using a Perkin Elmer TGA 4000 thermogravimetric analyzer. TGA thermograms of the coordination compounds were collected by heating the samples (which ranged from 1 to 10 mg) from 50 to 900 °C at a heating rate of 10 °C/min under a 100-mL/min nitrogen flow. The percentage weight loss was recorded against the temperature. Cyclic voltammograms were recorded on a CHI602E electrochemical analyzer using a three-electrode cell.

2.2. Synthesis of $[Cu(bim)_4Cl_2] \cdot 2H_2O$ (1)

An aqueous solution (20 mL) of $CuCl_2 \cdot 6H_2O$ (0.0025 M, 0.426 g) was added to a methanol solution (20 mL) of 1-benzylimidazole (0.01 M, 1.582 g) at a molar ratio of 1:4. The mixture was stirred for 4 to 5 h at room temperature, and then the resultant clear solution was filtered off and allowed to stand for crystallization. Dark blue crystals formed after a week and were analyzed by single crystal X-ray diffraction technique. Anal. Calcd for $C_{40}H_{44}Cl_2CuN_8O_2$: C, 59.81; H, 5.52; N, 13.95; Found: C, 58.62; H, 4.33; N, 11.26. mp = 135–148 °C. Yield = 83%.

2.3. Synthesis of $[Zn(bim)_2Cl_2]$ (2)

A DMF solution (20 mL) of $ZnCl_2$ (0.0025 M, 0.341 g) was added to a methanol solution (20 mL) of 1-benzylimidazole (0.01 M, 1.582 g) at a molar ratio of 1:4 and the mixture was stirred for 4 to 5 h at room temperature. Colorless crystals were obtained from the filtrate after a week and analyzed by single crystal X-ray diffraction technique. Anal, Calcd for $C_{81}H_{80}Cl_8N_{15}Zn_4$: C, 53.03; H, 4.45; N, 12.38; Found: C, 52.55; H, 4.48; N, 11.58. The mp of 162–174 °C is in the range of previously reported proposed complex [22]. Yield = 94%.

3. Results and discussion

General and spectroscopic characterization

3.1. IR analysis

Table 1 lists the FT-IR spectral analysis of the ligand benzylimidazole and its complexes, **1** and **2**. The infrared spectrum of the benzylimidazole ligand contains a prominent band at 3137 cm^{-1} , which can be attributed to N-H stretching vibrations. The IR band appearing at 1178 cm^{-1} can be assigned to N-C stretching of the benzylimidazole ring [24]. As evident from Table 1, the IR spectra of the ligand and the complexes contain peaks in a similar region. However, some significant variations are seen in the spectra of the metal complexes and their

free ligands. By comparing the infrared spectra of the free ligand with those of its complexes, the coordination modes and parts of the ligand bound to the metal ion were explored. On coordination, the stretching vibrations for the $\nu(\text{N-H})$ and $\nu(\text{C-N})$ bonds show a significant shift, with $\nu(\text{N-H})$ shifting from 3137 to 3122 and 3115 cm^{-1} , whereas $\nu(\text{C-N})$ shifted from 1178 to 1158 and 1150 cm^{-1} in metal complexes **1** and **2**, respectively. New characteristic peaks, which were absent in the spectrum of the ligand, were observed in metal complexes at 510 and 530 cm^{-1} , indicating M-N linkages [25] for complexes **1** and **2**, respectively.

<Table 1>

3.2. UV-visible absorption spectroscopy

Figure 2 shows the solid state UV-Visible spectra of the ligand and its complexes **1** and **2**. As evident from the spectrum of the free ligand, a prominent absorption band appears between 200 and 300 nm with maxima at 212, 234, and 270 nm; these may be assigned to the $\pi\text{-}\pi^*$ transitions of benzylimidazole [26, 27]. The absorption spectra of complexes **1** and **2** displayed different absorption patterns compared to that of the free ligand. The absorption bands observed with maxima at 335 nm in the spectrum of **1** and 211, 231, and 264 nm in the spectrum of **2** were assigned to the $\pi\text{-}\pi^*$ transitions of the imidazole group. Complex **1** exhibited broad and sharp absorption bands between 500 and 800 nm, which may be attributed to d-d transitions, a unique characteristic of transition metal ions (Cu^{2+}), whereas the spectrum of complex **2**, which has a d^{10} metal ion (Zn^{2+}) configuration, does not contain any peaks arising from d-d transitions [6]. The shifting of the absorption bands in the spectra of the complexes towards higher wavelengths for complex **1** and lower intensity for complex **2** is indicative of the metal ion coordination with the benzylimidazole ring.

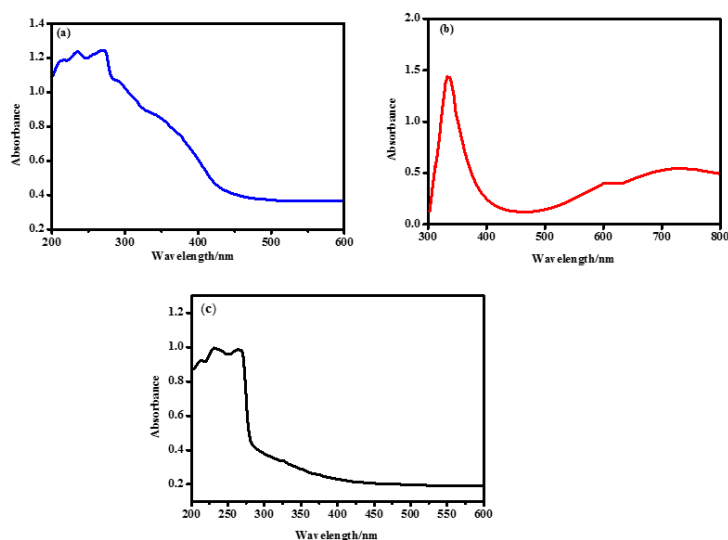


Fig.2. Solid state UV-Visible spectra of (a) free ligand (benzylimidazole), (b) complex **1** (c) complex **2**.

3.3. Fluorescence spectroscopy

Figure 3 shows the solid-state fluorescence emission spectra of the free ligand and its complexes, **1** and **2**, at ambient temperature. As obvious from the figure, the emission spectrum of the free ligand contains three significant emission peaks at $\lambda_{\text{max}} = 308, 367,$ and 420 nm upon excitation at 270 nm, and these may be assigned to the $\pi\text{-}\pi^*$ transitions of the delocalized π electrons in the imidazole ring and the $n\text{-}\pi^*$ transitions of the n -electrons of the nitrogen atoms of imidazole [28]. The emission spectrum of complex **1** contains two emission peaks at 375 and 497 nm upon excitation at 335 nm, whereas complex **2** displayed two emission peaks at 297 and 419 nm upon excitation at 264 nm. Comparing the emission spectral data of the free benzylimidazole ligand with those of its complexes, the emergence of new peaks in the emission spectra of the complexes can be attributed to the $\pi\text{-}\pi^*$ transition of the benzylimidazole ligands with metal ion charge transitions. In addition, there is fluorescence quenching in complexes **1** and **2**. The fluorescence quenching of a ligand by transition metal ions during complexation is a common phenomenon and can be explained by processes such as magnetic perturbation, redox activity, and electronic energy transfer [29-31]. On the formation of metal complexes, the energy of the ligand excited states, which are responsible for the emission spectrum, transfers to the metal ions, leading to a decrease in the fluorescence intensity [32].

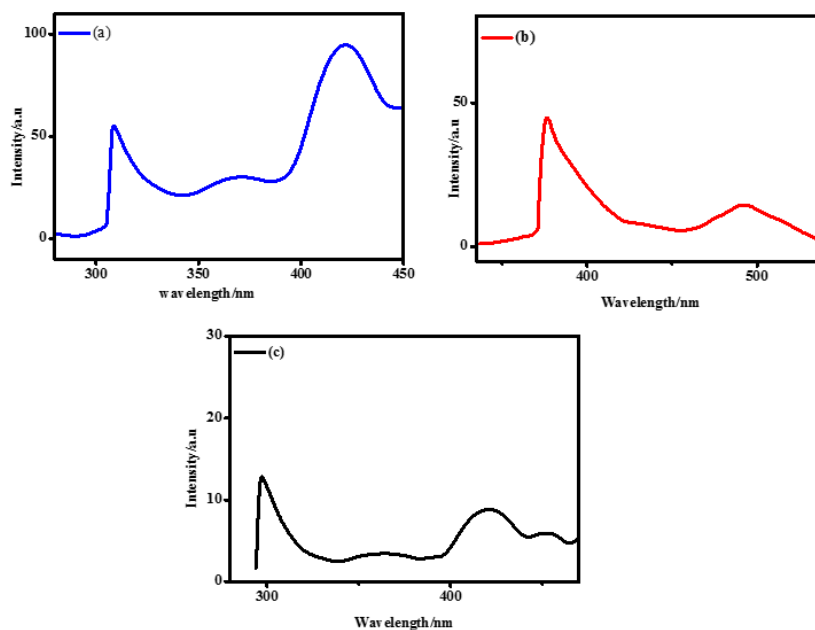


Fig. 3. Fluorescence spectra for (a) free ligand (benzylimidazole) (b) complex **1** (c) Complex **2**.

3.4. Crystal structure description

Complex **1** crystallized in the monoclinic space group $P2_1/c$. The crystal data and structural refinement parameters are shown in Table 2.

Complex **1** possesses one half-molecule with the center of symmetry at the Cu1 atom in the asymmetric unit, and the molecular structure is shown in **Figure 4a**. However, the octahedral geometry is due to the long-range interactions of Cu1 with the two Cl atoms occupying the axial positions. The Cu-Cl1 distances are 3.0897(7) Å. Similar observations has been observed in *catena*-poly[bis(1-methyl-1-tetrazole-κN4)copper(II)]-di-μ-bromo], in which the Cu-Br bond length is 3.101(4) Å [33]. The N2, N2A, N3, and N3A nitrogen atom of the imidazole rings occupy equatorial positions, with N2–Cu1–N3 and N2–Cu1–N3 bond angles of 86.94(7) and 93.06(7)°, respectively, making the geometry slightly distorted. The Cu1–N2 and Cu1–N3 bond lengths of 1.9887(17) and 2.0253(16) Å, respectively, are longer than that in [Cu(bhs)(Hdmpz)] (1.924(2) Å) [34]. Other bond length and angles are normal and comparable to the Zn complex

(Table 3). The cis imidazole rings, N1/N2/C8-C10 and N3/N4/ (C11-C13), are not coplanar but are twisted with an angle of 45.98° .

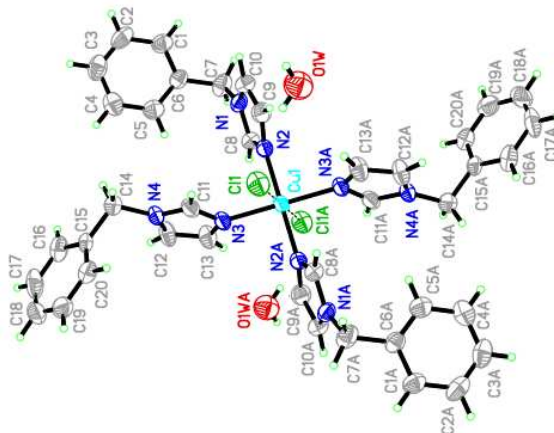


Fig. 4a. Molecular structure of complex **1**.

In the crystal packing structure of complex **1**, the interactions are dominated by C11-H11...Cl1 and intermolecular hydrogen bonds between the water molecules and chloride atoms, forming a two-dimensional network (**Figure 4b**). All the symmetry codes are given in Table 4.

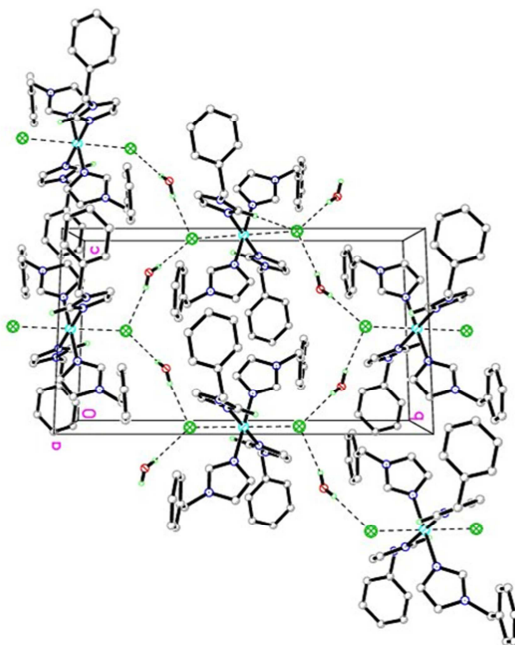


Fig. 4b. Crystal packing of complex **1** viewed down a axis. The dashed lines indicate hydrogen bond except chlorine to Cu atoms.

Complex **2** crystallized in the triclinic space group $P-1$. The asymmetric unit contains four crystallographic independent complexes. In the molecular structure of complex **2**, the Zn atom is coordinated by two nitrogen atoms (from two benzylimidazole ligands) and two chlorides, resulting in a tetrahedral coordination geometry (**Figure 5a**).

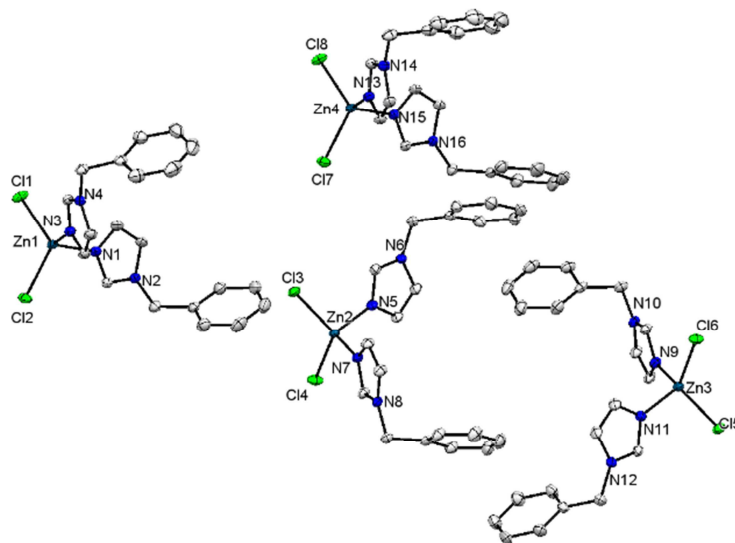


Fig. 5a. Asymmetric unit of complex **2**.

The two chloride atoms located at the basal position have Cl1-Zn1-Cl2, Cl3-Zn2-Cl4, Cl5-Zn3-Cl6, and Cl7-Zn4-Cl8 bond angles ranging from 117.45(2) to 119.87(2)°, while the two nitrogen atoms of the imidazole rings are in equatorial positions with N1-Zn1-N3, N7-Zn2-N5, N9-Zn3-N11, and N13-Zn4-N15 bond angles of 108.02(7) to 108.52(7)°, resulting in a significantly distorted tetrahedral geometry. The cis benzylimidazole rings are not coplanar. The Zn-N bond lengths (Zn1-N1, Zn1-N3, Zn2-N7, Zn2-N5, Zn3-N9, Zn3-N11, Zn4-N13, and Zn4-N15) range from 2.0022(17) to 2.0106(17) Å, and these are slightly shorter than those in $[\text{ZnCl}_2(\text{C}_{14}\text{H}_{12}\text{N}_2)_2]$, which have bond lengths ranging from 2.0048(17) to 2.0225(17) Å to the imidazole group [35, 36]. Other bond lengths and angles are within normal ranges (Table 3).

As shown in the crystal packing diagram, the intermolecular interactions are dominated by C-H...Cl and C-H... π interactions (blue dotted line), resulting in three-dimensional layers (**Figure 5b**). There are no classical hydrogen bonds in the structure.

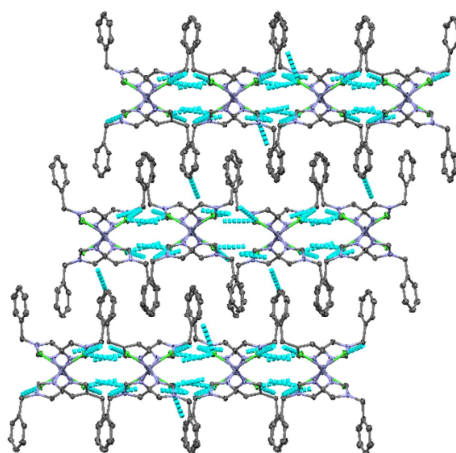


Fig. 5b. Crystal packing of complex **2** viewed down a axis.

<Table 2>

<Table 3>

<Table 4>

3.5. X-ray powder diffraction pattern

Figure 6 shows the experimental powder X-ray diffraction patterns for the Cu(II) and Zn(II) coordination complexes, which agree well with the simulated patterns calculated from the single crystal structures of complexes **1** and **2**, indicating that the samples are single phase and free from impurities.

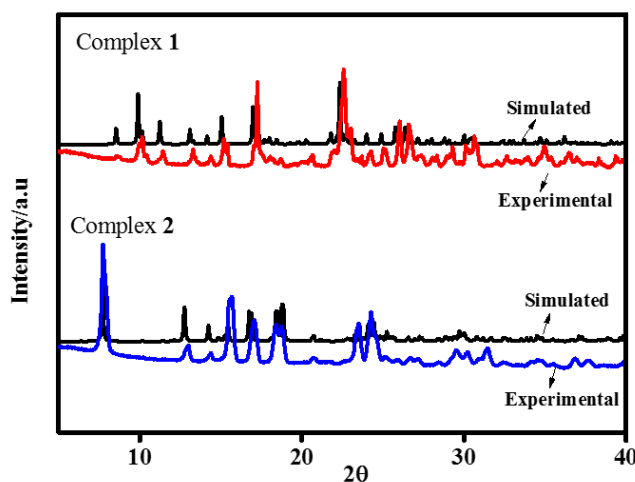


Fig.6. X-ray powder diffraction pattern of complex **1** and complex **2** (Black- simulated from CIFs, Red and Blue Experimental).

3.6. Thermogravimetric analysis

The results of TGA analysis for complex **1** and **2** are given in Table 5. The TGA and derivative thermal gravitational analysis (DTG) profiles (**Figure 7**) of complex **1** show a three-step degradation process with rapid weight losses of 3.6, 54.9, and 13.5% at 49.85–102.50, 135.41–298.85, and 486.43–731.05 °C, respectively, corresponding to the loss of the ligands, leaving 29% as the final residue. Based on the experimental method, the 29% residue is proposed to be Cu_3N_3 , which has a calculated percentage weight of 27.1%. The decomposition of complex **2** starts at 148.92–604.74 °C with an 88.1% weight loss, corresponding to the removal of all ligands. The calculated value of the end residue matched well with the proposed metallic zinc residue. Because of its high initial decomposition temperatures (greater than 148 °C), complex **2** is more thermally stable than complex **1**.

<Table 5>

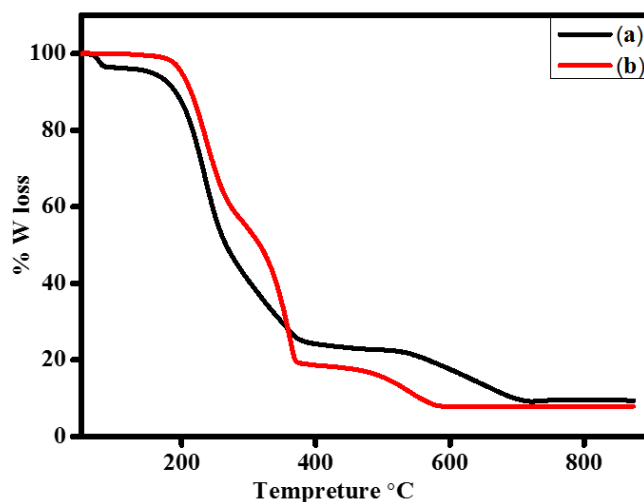


Fig.7. TGA Curve of (a) complex 1 (b) complex 2.

3.7. Electrochemical study

Electrochemical studies were performed for complexes **1** and **2**. Due to the different metal oxidation states, some redox properties are expected. Electrochemical measurements were carried out using a glassy carbon electrode in the presence of four different electrolytes: KCl, phosphate buffer, TRIS, and ammonium chloride (Table 6) at a scan rate of 50 mVs^{-1} . As shown in **Figure 8**, the peak potential separations ($E_{pc} - E_{pa}$) for complex **1** were 107, 93, 122, and 102 mV in KCl, phosphate buffer, TRIS, and NH_4Cl electrolyte solutions, respectively, and the ratios of cathodic current to anodic current I_{pc}/I_{pa} are 0.9, 0.86, 0.81, and 0.87, respectively, indicating that the redox reaction of the complex was quasi-reversible. Only one redox couple was detected for complex **1** using the previously mentioned conditions, which suggests that the cathodic peak is due to the reduction of Cu(II) to Cu(I). When the potential scan was reversed to positive potentials, anodic waves were observed at 0.01, 0.13, 0.12, and 0.15 V, respectively, indicating the oxidation of Cu(I) to Cu(II) [37]. In contrast, under the same condition, only one reduction peak was observed for complex **2**, which indicates that Zn(II) was reduced to Zn(0) at -0.68 V. The absence of an anodic peak in the reverse scan suggests that the reduced form of complex **2** is more redox stable.

<Table 6>

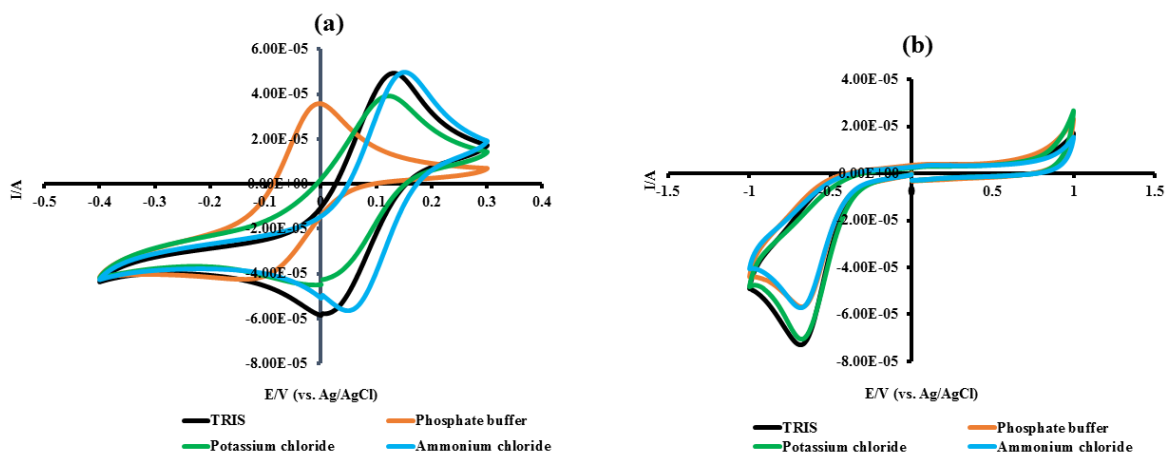


Figure 8: Cyclic voltammogram at a scan rate of 50 mVs^{-1} for (a) complex **1** (b) complex **2** using glassy carbon electrode (diameter = 2mm) in the presence 50mM KCl , phosphate buffer, TRIS, and ammonium chloride electrolyte solution. Scanning was performed against Ag/AgCl (sat.KCl) reference electrode.

4. Conclusions

We have successfully synthesized and structurally characterized two new coordination complexes $[\text{Cu}(\text{bim})_4\text{Cl}_2] \cdot 2\text{H}_2\text{O}$ (**1**) and $[\text{Zn}(\text{bim})_2\text{Cl}_2]$ (**2**). Spectroscopic techniques confirmed the metal-ligand coordination, and single X-ray diffraction results show that Cu(II) complex is octahedral geometry, while the Zn(II) complex is tetrahedral. Both complexes exhibit photoluminescence properties. In the electrochemical measurements, the voltammogram of complex **1** shows quasi-reversible redox reaction, while complex **2** shows only one reduction peak and no oxidation peak, arising from its stability in reduced form.

Supplementary material

CCDC No. 1478266 and 1519004 contains the supplementary crystallographic data for this paper. These data can be obtained free of charge from the Cambridge Crystallographic Data Center via http://www.ccdc.cam.ac.uk/data_request/cif.

Acknowledgements

Financial support from University Malaya of Research Grant (RP011B-14SUS), IPPP grant (PG116-2014B), High Impact Research Grants (UM-MOHE UM.C/625/1/HIR/MOHE/SC/09), Fundamental Research Grant Scheme, FRGS (FP005-2015A), UKM-Dip 2014-16 Research Grant and Higher Education Commission of Pakistan under FDP are acknowledged.

References

- [1] F. Hackenberg, M. Tacke, Benzyl-substituted metallocarbene antibiotics, and anticancer drugs, *Dalton Trans.*, 43 (2014) 8144–8153.
- [2] M. Salehi, G. Dutkiewicz, A. Rezaei, A. Amoozadeh, S. Rahmani, G.H. Grivani, M. Kubicki, Synthesis, antibacterial studies and crystal structures of tridentate Schiff base ligand and its cobalt(III) complex, *J. Chem. Crystallogr.*, 42 (2012) 871–878.
- [3] C.K. Prier, D.A. Rankic, D.W. MacMillan, Visible light photoredox catalysis with transition metal complexes: applications in organic synthesis, *Chem. Rev.*, 113 (2013) 5322–5363.
- [4] C. Parthiban, S. Ciattini, L. Chelazzi, K.P. Elango, Colorimetric sensing of anions by Cu(II), Co(II), Ni(II) and Zn(II) complexes of naphthoquinone-imidazole hybrid—Influence of complex formation on selectivity and sensing medium, *Sens. Actuators, B. Chem.*, 231 (2016) 768–778.
- [5] V.W.W. Yam, V.K.M. Au, S.Y.L. Leung, Light-emitting self-assembled materials based on d^8 and d^{10} transition metal complexes, *Chem. Rev.*, 115 (2015) 7589–7728.
- [6] M. Begum, E. Zangrando, M. Howlader, M. Sheikh, R. Miyatake, M. Hossain, M. Alam, M. Hasnat, Synthesis, characterization, photoluminescence and electrochemical studies of Ni(II), Cu(II), Zn(II), Cd(II) and Pd (II) complexes of the bidentate S-hexyl- β -N-(2-thienyl) methylenedithiocarbamate ligand, *Polyhedron.*, 105 (2016) 56–61.
- [7] Y. Wang, C. Zhang, H. Li, G. Zhu, S.S. Bao, S. Wei, L.M. Zheng, M. Ren, Z. Xu, Synthesis, characterization and in vitro anticancer activity of the biomolecule-based coordination complex nanotubes, *J. Mater. Chem. B.*, 3 (2015) 296–305.
- [8] T.W. Malone, K. Crowston, What is coordination theory and how can it help design cooperative work systems?. In *Proceedings of the 1990 ACM conference on Computer-supported cooperative work*, ACM, 1990, pp. 357-370.

- [9] J. Wang, A. Groeneveld, M. Oikonomou, A. Prusova, H. Van As, J.W. van Lent, A.H. Velders, Revealing and tuning the core, structure, properties and function of polymer micelles with lanthanide coordination complexes, *Soft Matter.*, 12 (2016) 99–105.
- [10] P. Sutra, A. Igau, Anionic phosph(in)ito (“phosphoryl”) ligands: Non-classical “actor” phosphane-type ligands in coordination chemistry, *Coord. Chem. Rev.*, 308 (2016) 97–116.
- [11] C.N. Tsai, S. Mazumder, X.Z. Zhang, H.B. Schlegel, Y.J. Chen, J.F. Endicott, Metal-to-ligand charge-transfer emissions of ruthenium (II) pentaammine complexes with monodentate aromatic acceptor ligands and distortion patterns of their lowest energy triplet excited states, *Inorg. Chem.*, 54 (2015) 8495–8508.
- [12] A. Duursma, R. Hoen, J. Schuppan, R. Hulst, A.J. Minnaard, B.L. Feringa, First examples of improved catalytic asymmetric CC bond formation using the monodentate ligand combination approach, *Org. Lett.*, 5 (2003) 3111–3113.
- [13] R. Brändén, B. Reinhammar, EPR studies on the anaerobic reduction of fungal laccase: Evidence for participation of type 2 copper in the reduction mechanism, *Biochim. Biophys. Acta, Protein Struct.*, 405 (1975) 236–242.
- [14] S. Nardecchia, D. Carriazo, M.L. Ferrer, M.C. Gutiérrez, F. del Monte, Three-dimensional macroporous architectures and aerogels built of carbon nanotubes and/or graphene: synthesis and applications, *Chem. Soc. Rev.*, 42 (2013) 794–830.
- [15] O. González-Ortega, R. Guzmán, Purification of human serum immunoglobulins using immobilized metal affinity chromatography with ethylenediamine triacetic acid as chelating agent, *J. Liq. Chromatogr. Relat. Technol.*, 38 (2015) 74–81.
- [16] C.F. Wu, W.Y. Chen, J.F. Lee, Microcalorimetric studies of the interactions of imidazole with immobilized Cu(II): Effects of pH value and salt concentration, *J Colloid Interface Sci.*, 183 (1996) 236–242.
- [17] A.Y. Kovalevsky, T. Chatake, N. Shibayama, S.Y. Park, T. Ishikawa, M. Mustyakimov, Z. Fisher, P. Langan, Y. Morimoto, Direct determination of protonation states of histidine residues in a 2 Å neutron structure of deoxy-human normal adult hemoglobin and implications for the Bohr effect, *J. Mol. Biol.*, 398 (2010) 276–291.
- [18] A. Kovalevsky, T. Chatake, N. Shibayama, S.Y. Park, T. Ishikawa, M. Mustyakimov, S.Z. Fisher, P. Langan, Y. Morimoto, Protonation states of histidine and other key residues in deoxy

normal human adult hemoglobin by neutron protein crystallography, *Acta Crystallogr., Sect. D: Biol. Crystallogr.*, 66 (2010) 1144–1152.

[19] A. Majumder, G.M. Rosair, A. Mallick, N. Chattopadhyay, S. Mitra, Synthesis, structures and fluorescence of nickel, zinc and cadmium complexes with the *N,N,O*-tridentate Schiff base *N*-2-pyridylmethylidene-2-hydroxy-phenylamine, *Polyhedron.*, 25 (2006) 1753–1762.

[20] D. Goodgame, M. Goodgame, G.R. Canham, Spectroscopic studies of substituted imidazole complexes. III. 2-methylbenzimidazole complexes of divalent cobalt, nickel, copper, and zinc, *Inorg. Chim. Acta.*, 6 (1972) 245–247.

[21] M. Maru, M. Shah, Transition metal complexes of 2-(substituted-1H-pyrazole-4-yl)-1Hbenzo[d]imidazoles: Synthesis and characterization, *J. Chem. Pharm. Res.*, 4 (2012) 1638–1643.

[22] C. Pettinari, F. Marchetti, A. Cingolani, S. Troyanov, A. Drozdov, Ligation properties of *N*-substituted imidazoles: synthesis, spectroscopic and structural investigation, and behaviour in solution of zinc(II) and cadmium(II) complexes, *Polyhedron.*, 17 (1998) 1677–1691.

[23] A. Bruker, Saint and SADABS, Bruker AXS Inc., Madison, Wisconsin, USA, (2005).

[24] S.A. Katsyuba, P.J. Dyson, E.E. Vandyukova, A.V. Chernova, A. Vidiš, Molecular structure, vibrational spectra, and hydrogen bonding of the ionic liquid 1-ethyl-3-methyl-1H-imidazolium tetrafluoroborate, *Helv. Chim. Acta.*, 87 (2004) 2556–2565.

[25] P. Jayaseelan, E. Akila, M.U. Rani, R. Rajavel, Synthesis, spectral characterization, electrochemical, anti-microbial, DNA binding and cleavage studies of new binuclear Schiff base metal(II) complexes derived from *o*-hydroxyacetophenone, *J. Saudi Chem. Soc.*, 20 (2013) 625–634.

[26] Y.H. Xing, J. Han, G.H. Zhou, Z. Sun, X.J. Zhang, B.L. Zhang, Y.H. Zhang, H.Q. Yuan, M.F. Ge, Syntheses and structures of mononuclear and binuclear transition metal complexes (Cu, Zn, Ni) with (salicylidene-glycine and imidazole), *J. Coord. Chem.*, 61 (2008) 715–730.

[27] H. Saral, Ö. Özdamar, İ. Uçar, Synthesis, structural and spectroscopic studies of two new benzimidazole derivatives: A comparative study, *J. Mol. Struct.*, 1130 (2017) 46–54.

[28] Z. Cheng, B. Yang, M. Yang, B. Zhang, Structural study and fluorescent property of a novel organic microporous crystalline material, *J. Braz. Chem. Soc.*, 25 (2014) 112–118.

- [29] U. Erkarslan, G. Oylumluoglu, M.B. Coban, E. Öztürk, H. Kara, Cyanide-bridged trinuclear Mn III–Fe III assembly: Crystal structure, magnetic and photoluminescence behavior, *Inorg. Chim. Acta.*, 445 (2016) 57–61.
- [30] A. Yasemin, Photoluminescence properties of Gd(III) and Ce(III) lanthanide-based metal-organic frameworks, *Acta Crystallogr., Sect. C: Struct. Chem.*, 72 (2016) 426–431
- [31] C. Hopa, I. Cokay, Designing a heterotrinnuclear CuII—NiII—CuII complex from a mononuclear Cu(II) Schiff base precursor with dicyanamide as a coligand: synthesis, crystal structure, thermal and photoluminescence properties, *Acta Crystallogr., Sect. C: Struct. Chem.*, 72 (2016) 601-606.
- [32] Z. Önal, H. Zengin, M. Sönmez, Synthesis, characterization, and photoluminescence properties of Cu (II), Co (II), Ni (II), and Zn (II) complexes of N-aminopyrimidine-2-thione, *Turk. J. Chem.*, 35 (2011) 905-914.
- [33] L.S. Ivashkevich, A.S. Lyakhov, M.M. Degtyarik, P.N. Gaponik, An X-ray powder diffraction study of catena-poly [[bis (1-methyl-1H-tetrazole- κ N4) copper (II)]-di- μ -bromo], *Acta Crystallogr., Sect E: Struct. Rep Online.*, 61 (2005) 394-396.
- [34] S. Paul, S.K. Bag, S. Das, E.T. Harvill, C. Dutta, Molecular signature of hypersaline adaptation: insights from genome and proteome composition of halophilic prokaryotes, *Genome Biol.*, 9 (2008) R70.
- [35] R. Bouhfid, E. Essassi, M. Saadi, L. El Ammari, Bis (1-benzyl-1H-benzimidazole- κ N3) dichloridozinc, *Acta Crystallographica Section E: Structure Reports Online*, 70 (2014) 94-95.
- [36] Y. Deng, Y. Zhao, X.D. Zhang, Y.S. Kang, W.Y. Sun, Coordination polymers with mixed 1, 3-bis (1-imidazolyl)-5-(imidazol-1-ylmethyl) benzene and multicarboxylate ligands: Synthesis, structure and property, *Microporous Mesoporous Mater.*, 231 (2016) 163-170.
- [37] M. Mamun, O. Ahmed, P. Bakshi, M. Ehsan, Synthesis and spectroscopic, magnetic and cyclic voltammetric characterization of some metal complexes of methionine: [(C 5 H 10 NO 2 S) 2 M II]; M II= Mn (II), Co (II), Ni (II), Cu (II), Zn (II), Cd (II) and Hg (II), *J.Saudi. Chemi. Soc.*, 14 (2010) 23-31.

Table 1. IR spectral data of ligand benzylimodazole and its complexes **1** and **2**.

Compound	$\nu(\text{N-H})$	$\nu(\text{C-N})$	$\nu(\text{M-N})$
Ligand (benzylimidazole)	3137	1178	-
Complex 1	3126	1158	510
Complex 2	3115	1104	530

Table 2. Crystal data and structure parameters for crystal complex **1** and complex **2**.

	1	2
CCDC No	1478266	1519004
Empirical formula	$\text{C}_{40}\text{H}_{44}\text{Cl}_2\text{CuN}_8\text{O}_2$	$\text{C}_{81}\text{H}_{80}\text{Cl}_8\text{N}_{15}\text{Zn}_4$
Formula weight	803.27	1808.68
Temperature/K	304(2) K	293(2)
Crystal system	monoclinic	triclinic
Space group	$P2_1/c$	$P-1$
$a/\text{\AA}$	10.9435(7)	12.3756(4)
$b/\text{\AA}$	17.8491(13)	14.5480(4)
$c/\text{\AA}$	10.5662(6)	24.7577(7)
$\alpha/^\circ$	90	106.590(2)
$\beta/^\circ$	109.201(2)	104.191(3)
$\gamma/^\circ$	90	90.275(3)
Volume/ \AA^3	1949.1(2)	4128.1(2)
Z	2	2
Density (calculated) / g/m^3	1.369	1.455
Absorption coefficient/ mm^{-1}	0.743	4.119
F(000)	838.0	1854.0
Crystal size/ mm^3	$0.430 \times 0.240 \times 0.160$	$0.3 \times 0.3 \times 0.3$
Theta range for data collection	3.0 to 28.3°	7.4 to 149.4°
Reflections collected	63639	28752
Independent reflections	4845 [R(int) = 0.0587]	16214 [R(int) = 0.0262]
Completeness to theta = 28.3°	99 %	99 %
Max. and min. transmission	0.8903 and 0.7405	0.088 and 1.000
Refinement method	Full-matrix least-squares on F^2	Full-matrix least-squares on F^2
Goodness-of-fit on F^2	1.062	1.005
Final R indices [$I > 2\sigma(I)$]	R1 = 0.0448, wR2 = 0.0927	R1 = 0.0409, wR2 = 0.1141
R indices	R1 = 0.0775, wR2 = 0.1067	R1 = 0.0470, wR2 = 0.122
Largest diff. peak and hole/ e.\AA^{-3}	0.23 and -0.88	0.77 and -0.78

Table 3. Selected bond lengths (Å) and bond angles (°) for complex 1 and 2.

Complex 1			
Atom	Length/Å	Atom	Angle / °
Cu1-N2	1.9887(17)	H(1WA)-O(1W)-H(1WB)	107(4)
Cu1-N3	2.0253 (16)	N(2A)-Cu(1)-N(2)	180.0
Cu1-Cl1	3.0897(7)	N2-Cu1-N3	86.94(7)
N(3)-C(1)	1.310	N2-Cu1-N3A	93.03(7)
Complex 2			
Atom	Length/Å	Atom	Angle/ °
Zn(1)-N(1)	2.0096(17)	N(1)-Zn(1)-N(3)	108.35(7)
Zn(1)-N(3)	2.0106(17)	N(7)-Zn(2)-N(5)	108.52(7)
Zn(1)-Cl(1)	2.2511(6)	N(9)-Zn(3)-N(11)	108.20(7)
Zn(1)-Cl(2)	2.2572(5)	N(13)-Zn(4)-N(15)	108.02(7)
Zn(2)-N(7)	2.0060(16)	Cl(1)-Zn(1)-Cl(2)	117.45(2)
Zn(2)-N(5)	2.0087(17)	Cl(4)-Zn(2)-Cl(3)	118.24(2)
Zn(2)-Cl(4)	2.2500(5)	Cl(5)-Zn(3)-Cl(6)	119.87(2)
Zn(2)-Cl(3)	2.2535(5)	Cl(8)-Zn(4)-Cl(7)	117.85(2)
Zn(3)-N(9)	2.0079(17)	N(15)-Zn(4)-Cl(7)	102.3(5)
Zn(3)-N(11)	2.0111(17)	N(1)-Zn(1)-Cl(1)	112.30(5)
Zn(3)-Cl(5)	2.2507(5)	N(7)-Zn(2)-Cl(4)	102.41(5)
Zn(3)-Cl(6)	2.2531(5)	N(9)-Zn(3)-Cl(5)	111.35(5)
Zn(4)-N(13)	2.0022(17)	N(13)-Zn(4)-Cl(8)	104.01(5)
Zn(4)-N(15)	2.0160(17)	N(3)-Zn(1)-Cl(2)	113.30(5)
Zn(4)-Cl(7)	2.2526(5)	N(5)-Zn(2)-Cl(4)	111.97(5)
Zn(4)-Cl(8)	2.2495(5)	N(11)-Zn(3)-Cl(6)	111.52(5)

Table 4. Hydrogen Bond (Å) for complex 1.

Complex 1				
D-H.....A	d(D-H)	d(H.....A)	d(D...A)	d(D-H.....A)
2O(1W)-H(1WA)...Cl1	0.82(2)	2.52(2)	3.293(3)	158(3)
2O(1W)-H(1WB)...Cl1	0.82(4)	2.65(4)	3.424(3)	158(4)
C(11)-H(11).....Cl1	0.93	2.77	3.462(2)	132

x,1/2-y,1/2+z

Table 5. TGA analysis for complex 1 and complex 2.

complex	Decomposition Range		Remaining Weight (%) Exp., (Calc.)	Expected Resides
	Temperature range (°C)	Weight loss (%)		
1	49.85 °C - 102.50 °C	3.6	29 (27.1)	Cu ₃ N ₂
	135.41 °C - 298.85 °C	54.9		
	486.43 °C - 731.05 °C	13.5		
2	148.92 °C - 290.48 °C	43.3	10.9 (14.3)	metallic zinc
	291.39 °C - 400.83 °C	35.4		
	423.87 °C - 604.74 °C	9.4		

Table 6. Electrochemical study Complex 1 and Complex 2 in different electrolytes solutions using glassy carbon electrode.

Complex 1	Glassy carbon		
Electrolytes	E _{P,A}	E _{P,C}	E _{1/2}
Phosphate buffer	0.00977	0.10254	0.05615
TRIS	0.13184	0.00977	0.07080
KCl	0.12451	0.01709	0.13794
NH ₄ Cl	0.15137	0.04883	0.10010
Complex 2	Glassy carbon		
Electrolytes	E _{P,A}	E _{P,C}	E _{1/2}
Phosphate buffer	No	0.67871	No
TRIS	No	0.68359	No
KCl	No	0.67627	No
NH ₄ Cl	No	0.68359	No

RESEARCH HIGHLIGHTS

- Synthesis of two new Cu (II) and Zn (II) coordination complexes with 1-benzylimidazole (bim) ligand; [Cu(bim)₄Cl₂].2H₂O (**1**) and [Zn(bim)₂Cl₂] (**2**).
- Characterization of the complexes by FT-IR, UV-Vis and fluorescence spectroscopic techniques, Powder and Single Crystal X-ray Diffraction Analysis and Thermogravimetric analysis.
- The complexes show redox properties due to different oxidation state of transition metal (Cu²⁺, Zn²⁺).